Investigation on Susceptibility to Hydrogen-Assisted Cracking in HSLA Steel Weldments

An area of maximum stress during phase transformation contributes to the susceptibility of hydrogen-assisted cracking

BY X. DI-JING, Q. HONG AND J. JIANMING

ABSTRACT. The effect of martensitic transformation stress on hydrogen-assisted cracking (HAC) initiation and propagation in high-strength steel HY-80 weldments was investigated using a new theory of martensite phase transformation.

The results calculated by a numerical computing program specially set up showed that the martensitic transformation stress was not uniformly distributed along the boundary of the martensite lath. The magnitude and nonhomogeneity of the distribution of the phase transformation stress increased significantly with the increase in prior austenite grain size. Consequently, there was a region of maximum phase transformation stress at the frontier of the fastest growing direction of martensite lath, and the susceptibility to HAC in this region increased rapidly.

It was found that the behavior of the initiation and propagation of HAC in augmented-strain cracking test specimens of high-strength HY-80 steel welded with the flux cored arc welding process (FCAW) correlates with the calculated results.

Introduction

It is well known that hydrogen-assisted cracking (HAC), which occurs between –100° to 200°C (–148°–212°F) in HSLA steel weldments, is basically dependent upon three mutually interactive factors: the amount of diffusible hydrogen in the weld, the level of the stress in the weld and the susceptible microstructure in the joint.

X. DI-JING is Professor, Chairman, and Q. HONG and J. JIANMING are Lecturers, Dept. of Metallic Materials Science and Engineering, Beijing Polytechnic University, Beijing, China.

The mechanism of cold cracking may be simply started from the mechanical aspect that a cold crack initiates while the stress and strain induced at a point reach critical values. But welding stress is rather complicated. Generally, the welding stress falls into three categories: thermal stress due to the nonuniform distribution of temperature, phase transformation stress and external restrained stress. The effect of the thermal stress and external restrained stress on HAC initiation and propagation was studied by many researchers. But little work was done on phase transformation stress. The role of phase transformation stress in HAC initiation and propagation remained unclear until now.

It was generally observed that the larger the grain size was, the higher the sensitivity to HAC. Many investigations showed that the threshold stress intensity levels, K_{Th} , below which neither stress-corrosion cracking nor HAC would occur, depended upon a number of variables, such as microstructure and grain size (Ref. 1).

KEY WORDS

Hydrogen-Assisted Cracking
Phase Transformation
HSLA Steels
HAC Susceptibility
Hydrogen Effects
Martensitic Transformation
Prior Austenite Grain
Crack Propagation
Heat-Affected Zone

Wood (Ref. 2) has suggested that the increasing grain size was the major variable most likely to affect the resistance to HAC in HSLA steels.

Easterling (Ref. 3) found that cold cracks initiated in the grain growth zone in HAZ and the increase of grain size effectively decreased the transformation temperature. So, in high-C_{eq} steels, the volume fraction of the lower temperature transformation products, such as martensite, bainite or Widmanstätten side laths (plate), increased. The high dislocation density associated with these products, together with fine carbide particle hardening, was thus likely to lead to a hard, low ductility matrix susceptible to HAC.

It is evident that the presence of twinned martensite is more dangerous than that of low-carbon martensite, and there is a certain relationship between the phase transformation and the susceptibility to HAC.

Christian (Ref. 4) suggested that the elastic energy of the phase transformation system uniformly distributed along the boundaries of the growing martensite lath. The assumption is contrary to some important phenomena of HAC.

Deng (Ref. 5) proposed a new theory for thermoelastic transformation, he suggested that the controlling factor of the phase transformation, in the radial and the thickening directions of the grain growth of martensite, is the localized equilibrium between chemical-free energy and the elastic energy in the growing frontier. Consequently, this theory provided the possibility for further study of the effect of martensitic transformation on HAC in the micro-area.

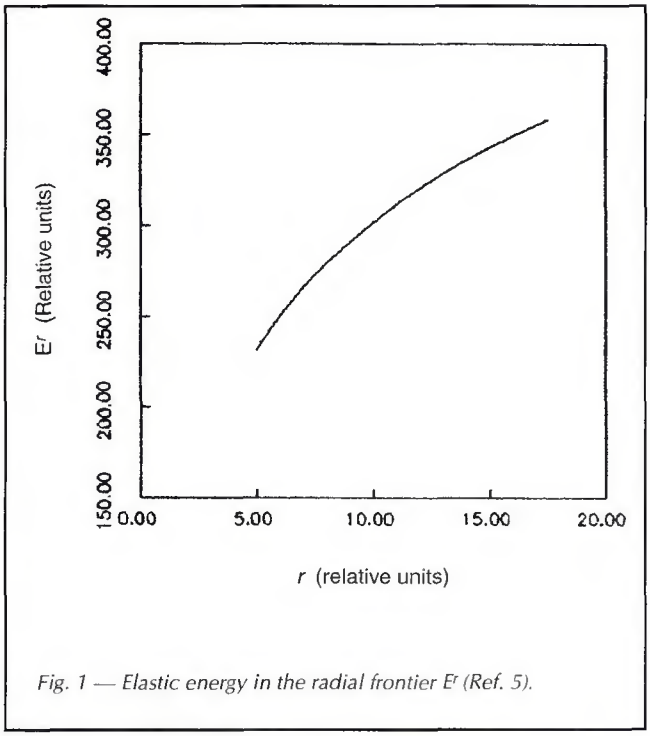

Fig. 1 — Elastic energy in the radial frontier E^r (Ref. 5).

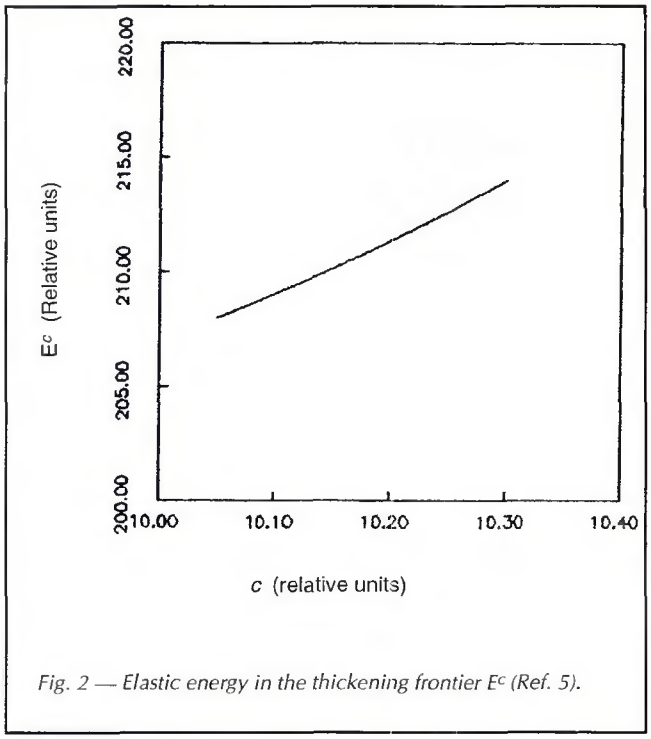

Fig. 2 — Elastic energy in the thickening frontier E^c (Ref. 5).

Theoretical Model and Calculation Formulas

A single growing martensite plate is under consideration. The cooling rate is slow enough that thermoelastic equilibrium can be reached at any temperature. The free energy change of the system ΔG is

$$\Delta G = \Delta G_{ch} + \Delta G_e + \Delta G_s + \Delta G_{ot}$$

where ΔG_{ch} is the change of chemical-free energy; ΔG_e is the change of elastic energy; ΔG_s is the change of interfacial energy; and ΔG_{ot} is the change of other kinds of energies, such as acoustic emission, external fields, and friction of the interphase boundary motion.

Among all these terms, the chemical-free energy and the elastic energy are the most important because the former is the driving factor for the transformation and the latter is the main hindering factor. The relationship between them basically determines martensite phase growth behavior. For a specific alloy composition, the change of total chemical-free energy depends on temperature and the volume of the martensite.

Estimation of elastic energy is much more difficult than that of chemical-free energy. Direct experimental measurements of elastic energy have not been reported, and the theoretical calculations depend strongly on the details of the model adopted. Average elastic energy can be used to calculate the elastic energy term in the formula above to estimate if a certain macroprocess is possible. But it is not suitable to describe the micro-process of martensitic transformation, and the distribution of elastic energy must be taken into account.

The essential assumption of the micro-area model for the martensitic transformation is that the controlling factor of the phase transformation, in the radial and the thickening directions of the growth of martensite, is the local equilibrium between chemical-free energy and the elastic energy in the growing frontier area, *i.e.*, the region near the interphase boundary. Esheby's continuum elasticity theory was chosen by Deng as the theoretical basis to calculate the local elastic energy (Ref. 5). According to the equations deduced by Deng, the elastic displacement tender at the growing frontier area caused by the martensite growth $U_i^c(r)$, can be written as the following formula, which is very convenient for numerical computing:

$$U_i^c(r) = \frac{1}{8\pi(1-\nu)} e_{jk}^T \int_v \frac{dv}{r^2} g_{ijk} \qquad (1)$$

where e_{jk}^T is elastic strain tensor in a free transformation, which is to be distinguished from the strain that occurs when the transformed region is constrained by the surrounding matrix.

$$g_{ijk}(1) = (1-2\nu)\left(\delta_{ij}l_k + \delta_{ik}l_j - \delta_{jk}l_i\right) + 3l_i l_j l_k$$

$$r = |r - r'| = \left[\sum_i \left(x_i - x_i'\right)^2\right]^{\frac{1}{2}}, \quad i = 1, 2, 3$$

$$l = (l_1, l_2, l_3)$$

$$l_i = \left(x_i - x_i'\right)/r \quad i = 1, 2, 3$$

The calculation of elastic energy, stress and strain in frontier area from the displacement is a standard procedure in elastic mechanics. Let e_{ij}^c be the strain tensor, then

$$e_{ij}^c = \frac{1}{2}\left[\frac{\partial u_i^c(r)}{\partial x_i} + \frac{\partial u_i^c(r)}{\partial x_j}\right] \qquad (2)$$

where,

$\frac{\partial u_i^c(r)}{\partial x_i}$ and $\frac{\partial u_i^c(r)}{\partial x_j}$ are the displacement components in different directions at the growing frontier area. Let σ_{ij}^c be the stress tensor, then

$$\sigma_{ij}^c = \lambda e_{ij}^c \delta_{ij} + 2\mu e_{ij}^c \qquad (3)$$

where λ is the lamé constant, and μ is the shear modules. Then, the change of elastic energy , G_e , is

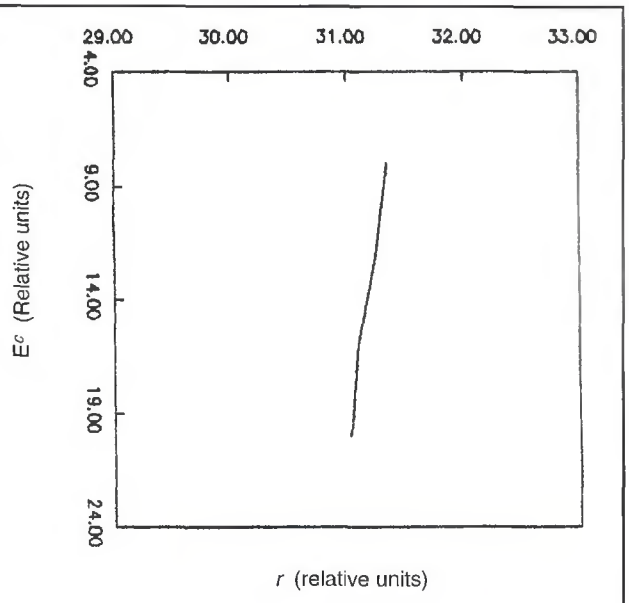

Fig. 3 — The relationship between E^c and r (Ref. 5).

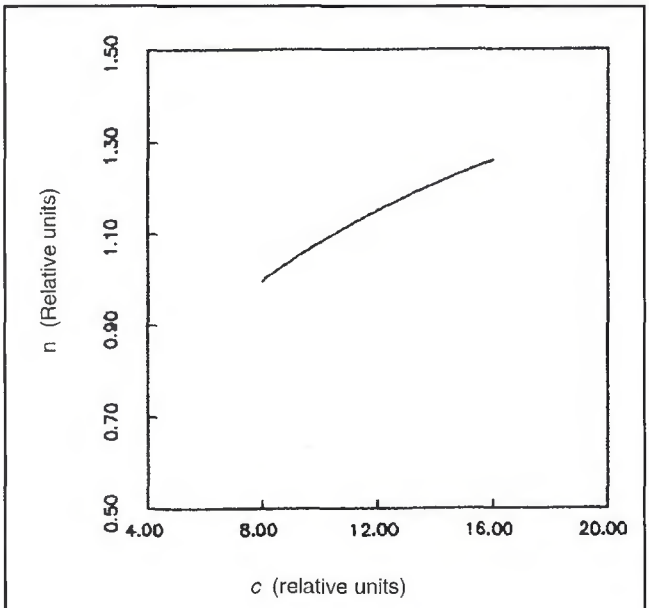

Fig. 4 — Nonhomogenous n changes with radius r (Ref. 5).

$$G_e = 0.5 \int_v e_{ij}^c \sigma_{ij}^c \, dv \quad (4)$$

The detail of the calculation procedure and the selection of the parameter was listed as Deng's computing program.

Calculation Results

The calculation of the local elastic energy in the radial growth frontier, E^r, and that in the thickening frontier, E^c, were done by Deng. Figures 1–4 show the calculated results.

Figure 1 shows the relationship between the elastic energy in the radial growth frontier area, E^r, and martensite radius, r, on conditions that a disk-shaped martensite is embedded in an infinite parent phase and its radius, r, is much larger than its semithickness, c, *i.e.*, r/c >100. These conditions are consistent with reported observations. Calculations on different shapes, including the oblate one, yields curves with the same tendency, *i.e.*, E^r increases with r increase.

Figure 2 shows that the local elastic energy in the thickening frontier area, E^c, increases with the increase of the semithickness of martensite lath, c.

It is worthwhile to notice the influence of radial growth on the local elastic energy in the thickening frontier area, *i.e.*, the relationship between E^c and r with a constant c. E^c is slightly reduced when r increases, as shown in Fig. 3. Generally, the growth velocity in the radial direction of martensite is different from that in the thickening direction, the former is much larger than the latter. Hence, the ratio r/c is very high. Thus, E^r will be much larger than E^c . This means that the elastic energy of the phase transformation system nonuniformly distributes along the growing boundaries of martensite lath. When n is the ratio of E^r to E^c , then n is an indicator of nonhomogeneity of the elastic energy distribution. Figure 4 shows the relationship between n and r; n goes up with the radial growth. The value of local elastic energy in the radial growing frontier of the martensite lath is higher than that in other areas.

The martensitic transformation stress is closely related to elastic energy of the transformation system. Since the value of local elastic energy in the radial growing frontier area of the martensite lath, *i.e.*, the martensite lath tip, is higher than that in other areas, the tip of the martensite plate or lath will become the region of the maximum martensitic transformation stress.

It has been confirmed that the possible maximum magnitude of martensite lath mainly depends upon the size of the prior austenite grain from which the martensite lath formed because martensite lath grows rapidly during the phase transformation process until it reaches the boundary of the prior austenite grain. Therefore, the prior austenite grain size determines the value of r and r/c of the martensite lath. It strongly affects the magnitude of the local elastic energy in the growing frontier of the martensite lath, as well as the nonhomogeneity of the elastic energy distribution. Obviously, the coarser the prior austenite grain, the larger is the phase transformation stress in the fastest growth direction, *i.e.*, the radial direction of the martensite lath, and the higher is the nonhomogeneity of the distribution of the phase transformation stress.

Calculation of the martensitic phase transformation stress of prior austenite of different grain sizes in high-strength HY-80 steel FCA welded was carried out by using a specially designed computer program in this investigation. Parameters for HY-80 are as follows:

Young's Modules: E = 200 GPa (2.04 x 10^6 kg/cm^2)

Shear Modules: μ = 74 GPa (0.75 x 10^6 kg/cm^2)

Poisson's Ratio: ν = 0.33

Normal Strain Component: $\xi_n = 0.09$

Shear Strain Component: $\xi_s = 0.19$

The habit plane of the lath martensite is close to {111}.

Calculated results listed in Table 1 show that the phase transformation stress increases significantly with the increase of the prior austenite grain size. Because of the great disparity in parameters of the material selected, it was difficult to calculate accurately the value of the phase transformation stress. Only the relative

Table 1 — Relationship between Martensitic Transformation Stress and the Prior Austenite Grain Size

Austenite grain size (relative units)	1	2	3	4	5	6	7	8	9	10
Martensitic transformation stress (relative units)	100	104	110	115	120	125	130	133	134	134

Table 2 — Chemical Compositions of the Base Metal and Undiluted Weld Metal

	C	Mn	P	S	Si	Ni	Cr	Mo
Base metal (HY-80 steel)	0.18	0.32	0.018	0.013	0.20	2.99	1.68	0.41
Undiluted weld metal (flux cored electrode E90T1-K2)	0.05	1.50	0.010	0.018	0.50	1.75	—	—

relationship between the phase transformation stress and the prior austenite grain size was found in this investigation. Table 1 reveals that the phase transformation stress will increase about 40% when the prior austenite grain size increases ten times.

Experimental Procedures

Base Metal and Filler Metal

An alloy-rich heat of HY-80 steel plate and an all-position flux cored electrode Dual Shield II E90T1-K2 were used in this investigation. The chemical compositions of the base metal and undiluted weld metal of the flux cored electrode E90T1-K2 are listed in Table 2. Figure 5 shows the microstructure of the base metal HY-80, which had been quenched in water and then tempered in air at 650°C (1202°F). The microstructure is tempered martensite.

Specimen Preparation and Experimental Procedure

The augmented-strain cracking (ASC) test samples and hydrogen content analysis specimens were cut from 38-mm (1.5-in.) plate. The welding parameters used in this investigation are listed in Table 3. The hydrogen content in the FCA weldment was increased by exposing the electrode to 100% humidity at 32°C (89.6°F) for several days. Both the ASC test and hydrogen content analysis procedures were the same as Savage's (Ref. 6).

Metallographic Examination

ASC test specimens were repolished and etched for metallographic examination to reveal the martensite microstructure and the prior austenite grain boundaries in the HAZ of the weldments.

Scanning electron microscopy analysis was carried out to examine the relationship among the initiation and propagation position of hydrogen-assisted cracking, the growth direction of the martensite lath, and the prior austenite grain boundaries.

Table 3—Flux Cored Arc Welding Parameters

Electrode diameter, in. (mm)	1/16 (1.6 mm)
Polarity	DCEP
Shielding gas	75%Ar-25%CO_2
Shielding gas flow rate, cfh L/min	35–40(16-19)
Electrode feed speed, in./min (mm/s)	210 (88.9)
Welding current, amperes (A)	200
Arc voltage, (V)	27
Travel speed, in./min (mm/s)	11 (4.66)
Heat input, kJ/in. (kJ/m)	29.5 (1161)

Experimental Results

Hydrogen-assisted cracking was observed in the ASC test specimens which had hydrogen content of more than 4 to 5 ppm and subjected to an augmented strain equal to or larger than 1.15% . Figure 6 reveals that the hydrogen-assisted cracking in the ASC test specimen initiated mainly in the HAZ at the grain boundaries of the coarse-grained prior austenite, and propagated into the weld metal or the base metal.

Scanning electron microscope (SEM) analysis of specimens demonstrated distinctly that the initiation and propagation positions of HAC were closely related to the growth direction of the martensite lath. A considerable number of observations revealed that HAC initiated often at the gathering region of the radial frontier of the martensite lath, *i.e.*, the gathering region at the tip of the martensite lath, at the coarse-grained prior austenite boundaries — Fig. 7. Frequently, the direction of HAC initiation and propaga-

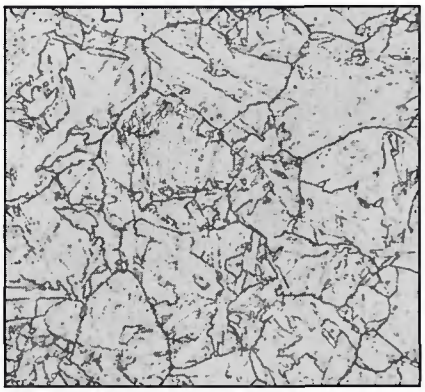

Fig. 5 — Microstructure of HY-80 base metal. Picric etch, 500X.

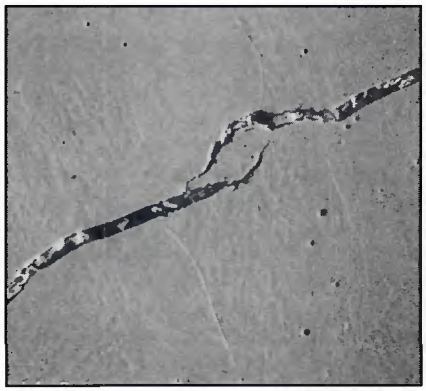

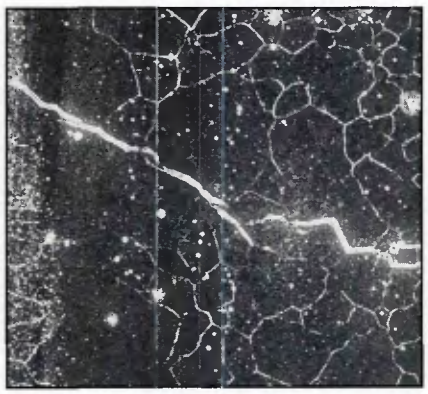

Fig. 6 — Hydrogen-assisted cracks. A — Initiated at the coarse-grained prior austenite boundaries in the HAZ, picric etch, 400X; B — propagated along the coarse-grained prior austenite boundaries, picric etch, 500X, SEM (BE).

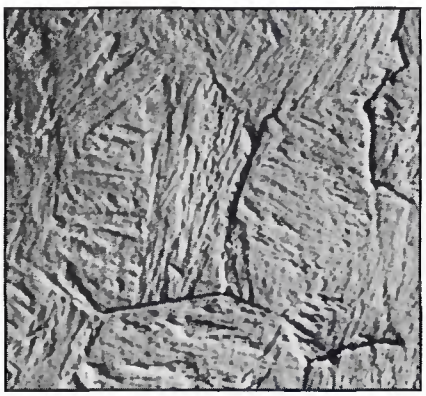

Fig. 7 — The relationship between HAC and the radially growing frontier of martensite lath, Vilella's etch, 100X, SEM (SE).

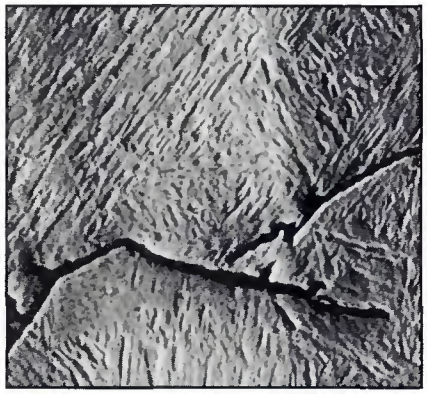

Fig. 8 — Relationship between HAC and the radially growing frontier of the martensite lath, Vilella's etch, 1000X, SEM (BE).

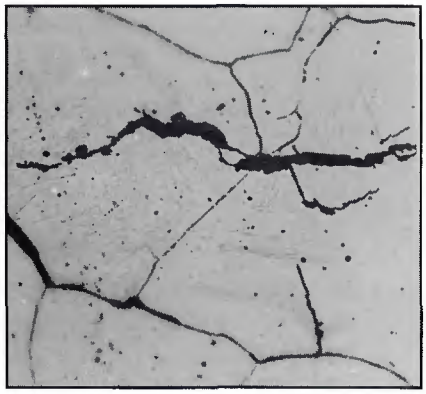

Fig. 9 — Hydrogen-assisted crack penetrated into the prior austenite grain, picric etch, 500X.

tion was roughly perpendicular to the radial direction of the martensite lath. The orientation of HAC would change if the direction of the martensite lath changed — Fig. 8.

Generally, the HAC occurred at the prior austenite grain boundaries, which were the thickening frontier of the growing martensite. Accidentally, HAC propagated through the prior austenite grains. The propagation would be diminished gradually — Fig. 9.

The size of the prior austenite grain size was estimated by the Intercept Method. The coarse-grained prior austenite had the ASTM grain size number of 3 (from 63.5 to 222 μm), and the prior austenite in the base metal and the fine-grained area of the HAZ had the ASTM grain size number of 7 (from 25.4 to 44.4 μm). This meant that the prior austenite grain size in the coarse-grained area in the HAZ increased 2.5 to 5 times as compared with the fine prior austenite. As described earlier in this paper, the possible maximum magnitude of the martensite lath was approximately equal to the size of the prior austenite grain.

Discussion

Experimental results indicated that the coarse-grained prior austenite boundaries along which HAC initiated and propagated were just the same as the fastest growing frontier (radial direction) of martensite lath, and were consistent with the region of calculated maximum martensitic transformation stress. For the HAZ investigated, the size of coarse-grained prior austenite is 2.5 to 5 times the grain size of the fine-grained prior austenite. According to the calculated result shown in Table 1, the martensitic transformation stress in the radial growing frontier of the martensite lath, at the boundary of the coarse-grained prior austenite, increases approximately 20% more than that at the boundary of the fine-grained prior austenite.

Although the martensitic transformation stress forms mainly at the interface of two phases, the parent prior austenite and the transformation product, martensite, the existence of the retained austenite will keep the stress until room temperature. In addition, at the prior austenite grain boundaries, phase transformation stress is in a very complex state because of the different orientation of the martensite lath in different prior austenite grains. Therefore, the martensitic transformation stress will not vanish after the transformation process.

Moreover, the orientation of the HAC initiation and propagation is usually perpendicular to the radial direction of the martensite lath, *i.e.*, perpendicular to the shear stress component of the martensitic transformation stress. It is considered that under the action of the shear stress component, the grain boundary will slip and vacancies will gather up at the grain boundaries. If the number of the vacancies reaches a certain level, the fissures will form and become the source of HAC initiation. The normal stress component of the martensitic transformation stress will add to the external stress and decrease the energy required and the critical size, r, for forming a platelet hydrogen cluster (Ref. 6). The experimental and calculated results described above fully proved that the martensitic transformation stress plays an important role in HAC initiation and propagation.

The nonuniform distribution of the phase transformation stress will lead to a nonuniform distribution of the diffusible hydrogen concentration. The larger the phase transformation stress is in a local area, the higher is the local hydrogen concentration. The maximum of the local hydrogen concentration will appear in the vicinity of the prior austenite grain boundary in the radial growing frontier of martensite lath, which is the region of the maximum phase transformation stress. Thereby, some parts of the prior austenite grain boundaries possess sufficient conditions for HAC initiation.

The increase in prior austenite grain size will also cause the Ms to decrease, and then the elastic energy and the local phase transformation stress to increase.

The phase transformation stress of high-carbon martensite is generally larger than that of low-carbon martensite because the high-carbon martensite has the higher carbon supersaturation level, the ratio of lattice constant c/a and the larger volume difference between martensite and austenite. Obviously, a high-phase transformation stress level must accompany the forming process of high-carbon martensite.

Of course, the HAC initiation and propagation processes are very complex. Other controlling factors for HAC initiation and propagation, such as external stress, local hydrogen concentration, the nonhomogeneity of the chemical composition, microstructure and the existence of micro defects, will affect the susceptibility to HAC.

The mechanics of the current HAC micromodel can be explained clearly from the sources of stress, considering the role of local martensitic transformation stress in HAC initiation and propagation. Some strange phenomena of the HAC with orientations that do not coincide with the macrostresses, *i.e.*, thermal stress and external restrained stress, can also be well explained.

Conclusions

Martensitic transformation stress is distributed nonuniformly along the martensite lath boundary. Its magnitude and nonhomogeneity increase with the increase of prior austenite grain size. There is a maximum region at the coarse-

grained prior austenite boundaries on the radially growing frontiers of the martensite laths.

The HAC in FCA welds on HY-80 steel initiated mainly in the region of maximum martensitic transformation stress in the HAZ.

The micromechanics of the current HAC initiation and propagation micromodel can be explained clearly from the sources of stress by using the theory of thermoelastic martensitic transformation.

Acknowledgments

This work was carried out mainly in the Dept. of Materials Engineering, Rensselaer Polytechnic Institute, Troy, N.Y. The authors extend their appreciation to Dr. G. S. Ansell, Dr. E. F. Nippes, and Metallographer N. J. Gendron for their enthusiastic help and support.

References

1. Gerberich, W. W., and Lessar, J. F. 1976. Grain size effects in hydrogen-assisted cracking. Metallurgical Transactions 7A: 953–960.

2. Wood, W. E., Das, K. B., and Parrish, P. A. 1977. The influence of microstructure on hydrogen embrittlement in high-strength steel. *Proc. of 2nd International Congress on Hydrogen in Metals*, Vol. 3.

3. Esterling, K. 1983. *Introduction to the Physical Metallurgy of Welding*, pp. 182–193, London, Butterworths.

4. Christian, J. W. 1965. *The Theory of Transformations in Metals and Alloys*, pp. 415–427 and 915–923, Oxford, Pergamon Press.

5. Deng, Y. 1985. A theory for thermoelastic martensitic transformation in Cu-Zn-Al alloys. Ph.D. dissertation, Rensselaer Polytechnic Institute, Troy, N.Y.

6. Savage, W. F., Nippes, E. F., and Husa, E. I. 1982. Hydrogen-assisted cracking in HY-130 weldments. *Welding Journal* 61(8): 233-s to 242-s.

7. Fujita, F. E. 1977. Theory of hydrogen-induced delayed fracture of steel. *Proc. of 2nd International Congress on Hydrogen in Metals*, Vol. 3, Oxford, U.K. Pergamon Press.

8. Coe, F. R. 1973. *Welding Steels without Hydrogen Cracking*, pp. 64–66, The Welding Institute, Abington, Cambridge, U.K.

9. Beachem, C. D. 1972. A new model for hydrogen-assisted cracking. *Metallurgical Transactions* 3(2): 259–273.